VII International Conference on Computational Methods in Marine Engineering
MARINE 2017
M. Visonneau, P. Queutey and D. Le Touzé (Eds)

Propulsion Performance Optimization of "Neighbour Duct" by CFD

Kenta Katayama*, Yoshihisa Okada*, Yasuo Ichinose† and Ryohei Fukasawa†

* Propeller design department, NAKASHIMA PROPELLER Co.,Ltd.
688-1, Joto-Kitagata, Higashi-ku, Okayama 709-0625, Japan
e-mail: ken-katayama@nakashima.co.jp, yoshihisa@nakashima.co.jp
web page: http://www.nakashima.co.jp

† Fluids Engineering and Hull Design Department, National Maritime Research Institute
6-38-1, Shinkawa, Mitaka-City, Tokyo 181-0004, Japan
e-mail: ichinose@nmri.go.jp, fukasawa@nmri.go.jp
web page: http://www.nmri.go.jp/index_e.html

Key words Energy-Saving Device, Duct, CFD, Optimization, EEDI.

Abstract. As one of measures against CO_2 reduction regulation by EEDI, energy-saving device (ESD) has been widely used. As one of ESD, the authors developed "Neighbour Duct" which was a vertical-long-oval stern duct.

Neighbour Duct generates thrust by harnessing flow along both sides of stern. By CFD, the geometric parameter of Neighbour Duct was optimized, and the principle of thrust generation was made clear.

In order to verify the result of CFD, a series of model test was carried out at National Maritime Research Institute (NMRI), the thrust deduction factors of both CFD and model test results were good agreement. As Estimation of performance of actual ship based on the model test, BHP was reduced 4.4% by Neighbour Duct. In addition, 1-w only decreased by 1%. Therefore it was found that CO2 reduction effect would be obtained by Neibour Duct without changing the propeller or propeller design.

1 INTRODUCTION

CFD (Computational Fluid Dynamics) has become large-scale year by year, and it has become possible to solve the flow field around the hull or the propeller accurately in the past few years. For this reason, CFD can be utilized to relatively easily develop energy-saving device.

Furthermore, as the demand for energy-saving has increased as a result of the increasing trend of international CO2 reduction such as EEDI regulation. Efficient method by CFD to develop energy-saving hull or device has been required.

Under such circumstances, the authors developed a stern duct by utilizing CFD. In the energy-saving device which is set in front of the propellers influences on the propeller revolution speed because of the operation point of the propeller changes. Therefore it is necessary to alter the design of propeller if the affect is large. Moreover, since the behavior of the bilge vortex is difference between the model and the actual ship, it must be to change the geometry of the energy-saving device [1]. However it is difficult to change the geometry of the device between the model and actual ship without numerous actual ship measurement

results.

In this study, thrust deduction coefficient 1-t was focused on and a duct which improved 1-t due to generate thrust was developed. The optimization method and CFD result of the duct was verified, the performance of the duct was evaluated.

2 DESIGIN OF "NEIGHBOUR DUCT"

2.1 Vertical-long-oval duct

Generally, in order to be generated thrust by a stern duct, it is necessary proper angle of attack of a stern duct against an upward flow or a downward flow due to a bilge vortex[2]. On the other hand, "Neighbor Duct" obtains thrust by harnessing flow along sides of hull, the duct has a vertical-long-oval shape so as to be along sides of the hull as much as possible.

The shape of the duct was defined by several parameters, and optimization calculation using CFD was performed while changing the parameters.

2.2 Optimization by CFD

2.2.1 Particulars of the hull and propeller

In the optimization, 82,000 DWT Panamax bulk carrier developed by NMRI was used as the target ship. Principal particulars of the hull are shown in Table 1, and the propeller particulars are shown in Table 2. In this study, CFD was carried out on the model scale in order to verify by model test.

Table 1: Principal particulars of hull

NMRI 82Pana_Max Bulk Carrier			
Condition		Designed Full	
Principal Dimension		Actual	Model
Length Between Perpendiculars	[m]	222	7.631
Length on Designed Load Water Line	[m]	225	7.734
Breadth	[m]	32.26	1.109
Depth	[m]	19	0.653
Design Draft	[m]	12.2	0.419
Block Coefficient		0.87	0.87

Table 2: Principal particulars of propeller

Principal Dimension		Actual	Model
Diameter	[m]	6.4	0.22
Pitch Ratio		0.6781	0.65
Boss Ratio		0.16	0.16
Expanded Area Ratio		0.495	0.55
Chord Length at 0.7R	[m]		0.0696
Number of Blades		4	4
Shaft Center Line Height	[m]	3.5	0.1203

2.2.2 Calculation condition

In this study, SC/Tetra which is a commercial code was used for CFD. The calculation was used the double-body model, and the turbulence model was SST k-ω. Fig.1(a) shows the calculation domain, and (b) the state of mesh around the stern.

In the calculation domain, a hull model is placed in a semi-cylindrical watershed, the dimensions of the calculation area are based on the Length of perpendicular (Lpp) of the hull model. The distance from the inlet to the bow equals Lpp, the radius of the cylinder equals Lpp, the distance from the stern to the outlet is twice of Lpp. The propeller thrust and torque were obtained on the propeller disk in Fig.1(b) by infinitely blade propeller theory.

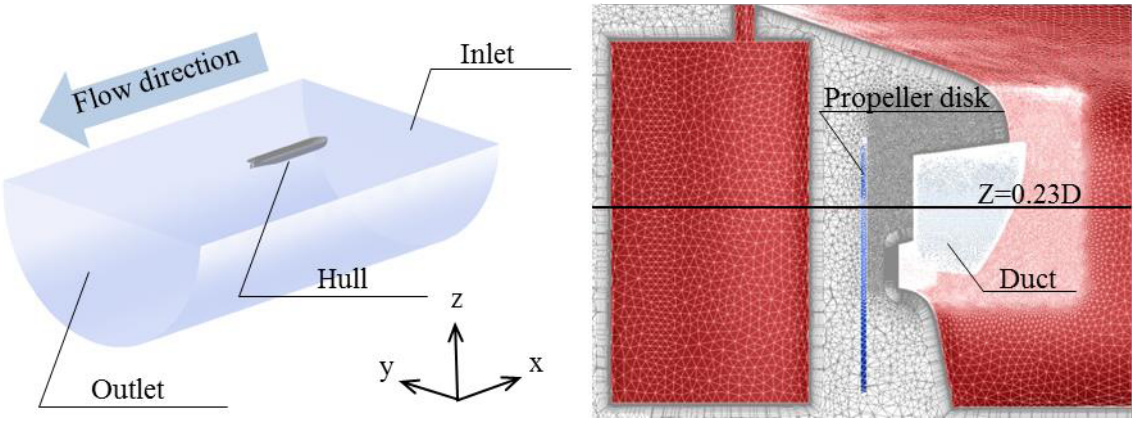

Figure 1: (a)Overview of the calclation domain, (b)The mesh around the stern

The computational grids were mainly unstructured tetrahedral grids, and the prism grids were used in the boundary layer. The overset grid approach is used for the duct. The grids around the duct are subdivided in order to improve accuracy of the calculation.

The total number of cells was 32.6 million, and the dimensionless distance y+ from the wall surface of the first layer of the boundary layer was 1 or less.

The coordinates are the center point of the propeller disk as the origin, the x axis in the bow direction, the y axis in the port direction and the z axis in the water surface direction.

In the calculation of self-propulsive condition, calculation at 3 different revolution speeds of propeller was performed at design ship speed, and the self-propulsion factor at the self-propulsion point was obtained by interpolation.

The hull resistance was calculated without the duct. This resistance was used regardless with or without of the duct when calculate of the self-propulsion factor. Since the double-body model is applied to stabilize the calculation, the wave resistance is evaluated by the tank test results, which obtained from the resistance test conducting at the 400 m towing tank at NMRI.

2.2.3 Optimization

For optimization, self-propulsion factor was calculated for each duct which has difference shape parameter. The ratio of 1-t, 1-w with and without the duct are assumed to be $\triangle$1-t, $\triangle$1-w. The performance of the duct was evaluated of the two values, and other factors were not considered.

Fig.2(a) shows the calculation results. The vertical and the horizontal axis represent ⊿1-w and ⊿1-t to plot the values obtained in each self-propulsion calculation on the chart. At the point painted red in Fig.2(a), ⊿1-t is 2.6% and ⊿1-w is -2.9%, and the shape at this point is decided as the optimized duct. Fig.2(b) shows the geometry of the optimized duct.

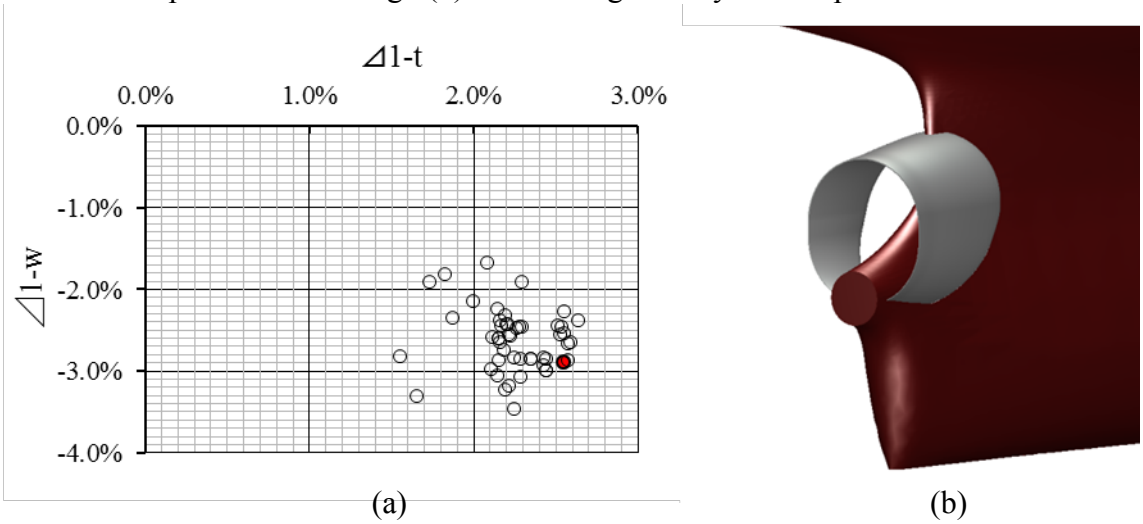

Figure 2: (a) The optimization result, (b) the geometry of the optimized duct

In the geometric parameters of the duct, having a large influence on the self-propulsion factor were size of the duct, opening angle of the duct and the side projection shape of the leading edge of the stern duct. The side projection shape of the leading edge has a large influence on 1-t. From those, it was found that the mutual position of the leading edge of the duct and the side of the hull is important.

3 PRINCIPLE OF THRUST GENERATION BY "NEIGHBOUR DUCT"

3.1 Analysis flow field around the duct

The principle of thrust generation was analyzed in the optimized duct by CFD in detail.

As Dp is the propeller diameter, and a plane is put on Z = 0.23 Dp as shown in fig.1(b). Fig.3 shows the streamlines and the pressure distribution on the inspection plane in the state with and without the duct. The streamline passes through a point on the inspection plane indicated by purple 'x' mark in fig.3.

As shown in the stream line and the pressure distribution on the plane, the flow along the hull sides flows to the duct with proper angle of attack. Therefore the lift is generated in the duct and thrust is generated. However, since the inside of the duct becomes negative pressure, drag occurs to the stern.

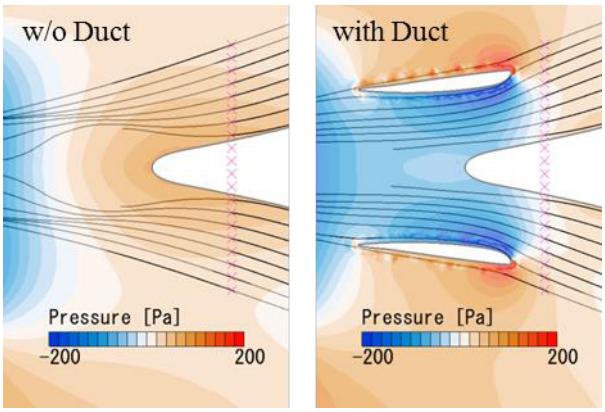

Figure 3: The stream line and the pressure distribution on a plane

3.2 Pressure analysis on hull and stern duct surfaces

In order to evaluate the force exerted by the pressure in the state of with and without the duct, the normal vector of each surface was multiplied by pressure, and the x direction component Px of them was obtained.

Fig.4(a) shows the distribution of Px on the surface of the hull in the state of with and without the duct. A positive value represents thrust and a negative value represents resistance.

Comparing Px distribution with and without the duct, Px turns from positive to negative in the region where the surface of the hull is covered with the duct, which indicates that the resistance increased on the surface of the hull with the duct.

On the other hand, at the distribution of Px on the surface of the duct shown in fig.4(b) shows a positive value as a whole, and in particular, it can be found that a large thrust is generated at the leading edge from the side portion to the upper portion inside the duct.

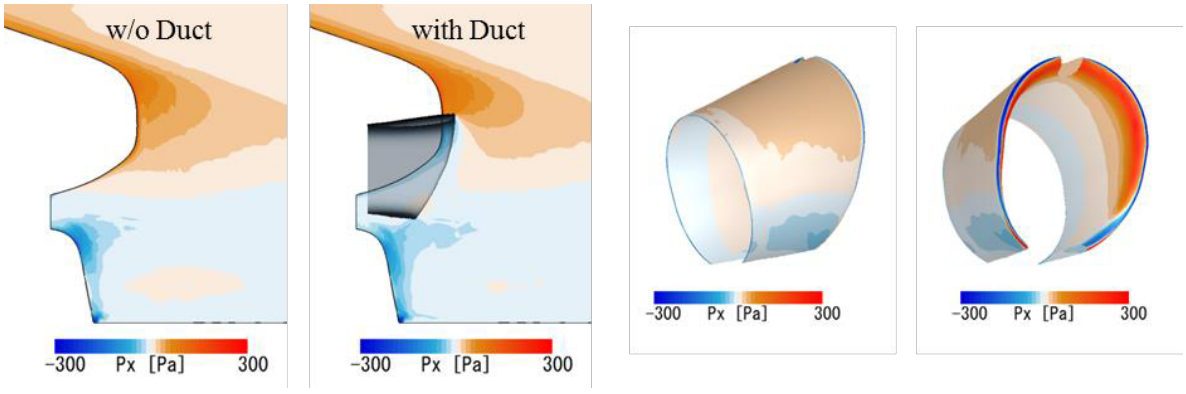

(a) (b)

Figure 4: (a)Px distribution on hull surface, (b)Px distribution on duct surface

3.3 Change in thrust by stern duct

In order to compare the resistance and the thrust by the duct, the force Fx which working on the surface of the hull and the duct is obtained from integration Px. Each Fx is shown in Table 3. However, due to the change the flow into the propeller by the duct, the propeller

wake flow changes and the resistance value of the rudder changes. The authors focused only on the relation between the hull and the duct, not including the rudder.

From Table 3, it can be found that the thrust generated by the duct is larger than the hull resistance. Therefore the thrust is increased in whole. Since trade-off between hull resistance and duct thrust is important for increasing thrust, it is clear that the mutual position of the duct and hull becomes important. This confirms the finding that the influence of the mutual position of the leading edge of the duct and the side of the hull obtained by the optimization calculation is large.

Also, the front edge of the duct side part generates a large thrust and it can be said that increasing the thrust generating part using the vertical-long-oval shape is effective for improving thrust.

Table 3: The differnce of Fx by the duct

Region		Hull	Duct	Total
Fx : without duct	[N]	-14.36	-	-14.36
Fx : with duct	[N]	-14.58	0.63	-13.95
Difference	[N]	-0.22	0.63	0.41

4 MODEL TEST

4.1 Model

In order to verify the results obtained by the optimization calculation, a towing tank test was conducted in a 400 m water tank at NMRI. Regarding the resistance value used for the self-propulsion test, the resistance test value without stern duct was used as a reference regardless of the presence or absence of the duct was same as CFD. Fig.5 shows a photograph around the stern of the model used in the test. The model of the duct was made of resin and made with a 3D printer.

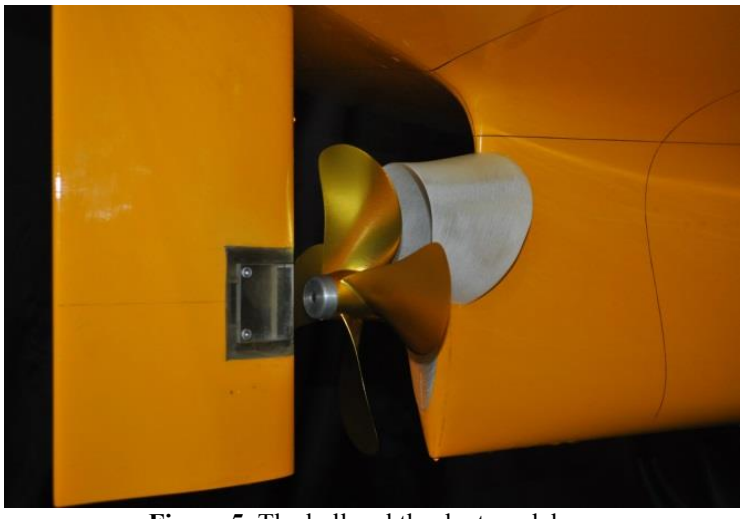

Figure 5: The hull and the duct model

4.2 Comparison between model test and CFD

4.2.1 Self propulsion factor

Fig.6 shows 1-t and 1-w obtained from CFD and model test at design speed. According to the model test result, ⊿1-t and ⊿1-w are 2.7% and -0.9%, respectively. Comparing CFD with the results of the model test, the absolute values of 1-t and 1-w are somewhat different, but the trend is consistent. Although ⊿1-t is a reasonable calculation result, it proved to be overestimating about ⊿1-w.

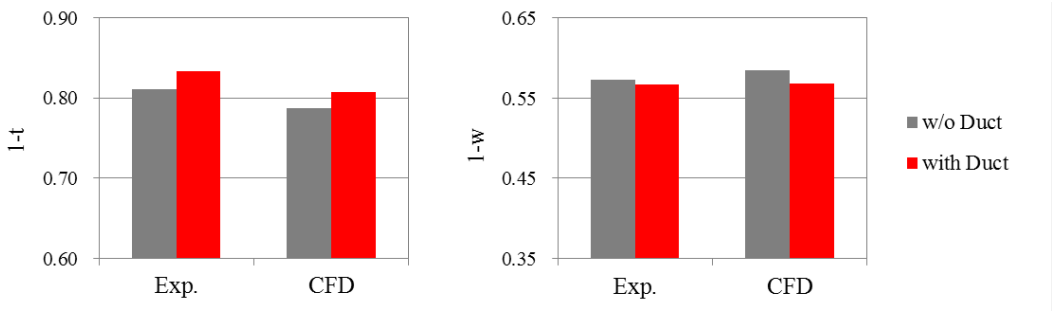

Figure 6:Comparison of self-propulsion factor

4.2.2 Wake distribution

Fig.7 shows the wake distribution obtained from the CFD and the model test. Comparing the CFD and the result of the model test without the duct, the position of the bilge vortex center and the state of the downwash by the vortex are in good agreement with each other. However at the upper middle part of the propeller disk, 1-w of the CFD result was lower.

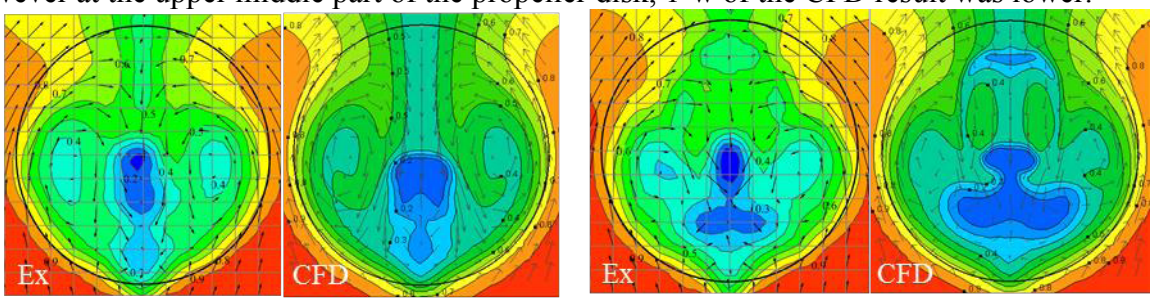

(a) (b)

Figure 7: Comparison of wake distribution (a)without the duct, (b) with the duct

Also, looking at the difference between the two due to the presence or absence of a stern duct, the change of wake by the stern duct is similar, but the degree of decrease of 1-w behind the stern duct is larger for CFD.

From these results, it can be said that this calculation method tends to evaluate excessively the deceleration degree of the fluid behind the object, such as a stern end and a stern duct. Therefore, the self-propulsion calculation by CFD seems to overestimate difference of 1-w due to the presence or absence of the duct.

5 THE PREDICTION OF PERFORMANCE OF THE ACTUAL SHIP

The performance of the actual ship was predicted based on the model test results. EHP was calculated by three-dimensional extrapolation method from the resistance test result without the duct. The wake coefficient correction 1-Ws with the duct was obtained from Yazaki chart and the following equation[3].

$$1 - W_S = \varepsilon_0 \times (1 - W_{T0}) - \Delta w \tag{1}$$

$$\varepsilon_0 = (1 - W_S)/(1 - W_T) \tag{2}$$

$$\Delta w = (1 - W_{T0}) - (1 - W_T) \tag{3}$$

W_{T0}: Wake factor without a duct
W_T: Wake factor with a duct
Δw: Influence to wake factor by a duct
ε_0: Wake correction factor without a duct

Table 4: The prediction of performance of the actual ship

Condition	Design Draft	
Vs (Knot)	14.2	
Fn	0.1555	
Duct	w/o duct	with duct
EHP (kW)	5,327	5,327
η_R	0.979	0.987
1-t	0.811	0.833
1-W_T	0.573	0.567
1-Ws	0.627	0.621
η_H	1.294	1.341
ηos	0.524	0.525
ηs	0.663	0.694
BHP (kW)	8,112	7,752
Ns (RPM)	114.7	113.4

The performance prediction of the actual ship estimation results are shown in Table 4.

Effects on each self-propulsion factor by the duct on the actual ship were improved by 2.7% for 1-t, 1% for 1-Ws, 0.9% for ηr and 0.2% for ηo respectively, and BHP is reduced 4.4%. The change amount of 1-Ws is relatively small, therefore there is little influence on the propeller operating point, it can be said that it is not necessary to change the propeller design greatly.

6 CONCLUSION

In this study, we developed “Neighbour Duct”, for generating thrust by harnessing flow along sides of hull, and optimization of the geometric parameters of the duct were carried out by utilizing CFD.

Comparison the presence or absence of the duct, 1-t and 1-w were improved by 2.6% and 2.9% respectively in the result of CFD.

It was found that not only the size and opening angle of the duct but also the mutual position of the leading edge of the duct and the sides of the hull influences the duct performance.

In the model test, 1-t and 1-w were improved by 2.7% and 0.9% respectively by the duct. Comparison the model test and the CFD result, the result of 1-t is a reasonable, however 1-w seems to be overestimate in CFD because of the flow behind the object is excessively decelerated. In this study, although 1-t and 1-w were evaluated equally in optimization, it seems that an evaluation method weighting 1-t is more appropriate.

Analysis of the principle of thrust increase of the duct using the CFD result showed that by setting the duct having proper angle of attack regarding to the flow of the side portion of the hull, thrust was found to occur. Therefore, a vertical-long-oval duct which increases the thrust generating part on the side seems to be considered effective for efficiency improvement.

The performance of the actual ship was predicted based on the model test results and it was found that the duct reduces BHP of 4.4%. In addition, it is found that 1-w was only decreased 1%. Therefore

The wake flow distribution near the top changes by the duct, therefore it would be considered the influence on cavitation and surface force. In addition, it is necessary to accurately estimation method of the flow behind the duct in order to consider the influence of cavitation by CFD.

ACKNOWLEDGMENTS

In conducting this research, Dr. Yasutaka Kasahara and Dr. Yusuke Tahara of National Maritime Research Institute provided valuable guidance and advice. I would like to express my sincere gratitude.

REFERENCES

[1] Y. Inukai et al., “Energy-Saving principle of the IHIMU semicircular Duct and Its Application to the Flow Field Around Full Scale Ship”, IHI Engineering Review., Vol. 50, No.4 pp. 33-38, (2010).

[2] Universal Shipbuilding Co.,Ltd., “Stern Duct and Ship equipped it”, Japan patent 2008-24072, (2008).

[3] H. Kawashima et al., “Study of Weather Adapted Duct (WAD)”, Papers of National Maritime Research Institute, Vol. 14, No.2 pp. 89-104, (2014).